Int. J. Electrochem. Sci., 6 **(2011)** 6165 - 6176

International Journal of
ELECTROCHEMICAL
SCIENCE
www.electrochemsci.org

Preparation of $Li_5Fe_{1-x}Mn_xO_4$ /CNT Materials for Li-Ion Batteries

Keqiang Ding[1,2], *Li Wang*[1,*], *Jianjun Li*[1], *Haitao Jia*[2], *Xiangming He*[1]

[1] Institute o f Nuclear & New Energy Technology, Beijing Key Lab of Fine Ceramics, Tsinghua University, Beijing 100084, China
[2] College of Chemistry and Materials Science, Hebei Normal University, Shijiazhuang, Hebei 050016, P.R. China
[*]E-mail: wang-l@tsinghua.edu.cn

Received: 23 July 2011 / *Accepted:* 28 October 2011 / *Published:* 1 December 2011

A proposed two-step solid-state process is attempted to prepare $Li_5Fe_{1-x}Mn_xO_4$/carbon nanotubes (CNTs) materials for Li-ion batteries. The process includes the following steps. A mixture containing $Fe(NO_3)_3$•$9H_2O$, $LiOH$•H_2O and $Mn(CH_3COO)_2$·$4H_2O$ is thoroughly ground leading to a fine powder, and then this mixture is sintered at 470 °C for 10 h , followed at 750°C for 3h. To improve the conductivity of the obtained samples, carbon nanotubes (CNTs) are incorporated into the precursor, generating composite/CNTs $Li_5Fe_{1-x}Mn_xO_4$. The obtained samples are featured by FTIR, X-ray diffraction (XRD), scanning electron microscope (SEM), and their electrochemical performances are investigated. It is revealed that the incorporation of CNTs can greatly enhance the electrochemical performance of $Li_5Fe_{1-x}Mn_xO_4$. More interestingly, the phenomenon that the CNTs incorporation can significantly influence the particle size of obtained samples is observed in this study.

Keywords: lithium battery, Li_5FeO_4, manganese(Mn) doping; carbon nanotubes.

1. INTRODUCTION

Of late, except for the commercial cathode materials (for instance, $LiCoO_2$ and $LiMn_2O_4$), many novel cathode materials such as $LiFePO_4$ and $LiMnPO_4$, and etc., have been successfully developed, but their flaws are also revealed step by step [1]. Thus, preparing novel cathode materials is still the main task especially for the electrochemical researchers [2]. With the development of investigation on cathode materials, metal doping is regarded as a feasible way to enhance the electrochemical performance of cathode materials. Many kinds of metals, such as Ag [3], Mg [4], Ti, [5], Mg [6], Cu [7], and etc, have been doped into cathode materials with an intention to get an improved electrochemical behavior. As one typical metal element, manganese (Mn) is also doped into

cathode materials. For example, Ahn [8] doped Mn into $LiFePO_4$, and reported the synthesis of $LiMn_{0.4}Fe_{0.6}PO_4$ (LMFP) prepared by a sol–gel technique using citric acid as foaming agent and carbon precursor, and he addressed that a composite that shows the better electrochemical performance has more porous structure. Lee [9] described the synthesis of $LiFe_{0.6}Mn_{0.4}PO_4$ using a solid-state reaction of $(Fe_{0.4}Mn_{0.6})_3(PO_4)_2$ and Li_3PO_4 mixed at a molar ratio of 1:1, with the addition of stearic acid as the carbon source to increase conductivity, and demonstrated with XAFS characterization that initially delithiated Fe-rich domains at 3.5V can promote more effective local structural change of the neighboring Mn-rich domains during the next second plateau at 4.1V, which can ease delithiation in the Mn-rich domains through more flexible reaction of the local structure in the Mn octahedra. Capsoni [10] investigated the doping of Mn in $Li_3V_2(PO_4)_3$, and addressed that the Mn doping improves the electrochemical features with respect to the undoped samples, and explained that the Mn substitution on both the V sites can enhance the capacity slightly in the sol–gel synthesis, while in the solid state synthesis the significant capacity enhancement is preferentially due to the microstructural features of the crystallites and to the $LiMnPO_4$ phase formation. Saadoune [11] systematically discussed the synthesis, the crystal structure and the study of the structural changes during the electrochemical cycling of layered $LiNi_{0.1}Mn_{0.1}Co_{0.8}O_2$ positive electrode material.

As a kind of cathode material, Li_5FeO_4, containing only three elements, has also been paid attention as far as in 1971. For instance, Demoisson et al. have developed new Lithium iron oxides, i.e., high temperature and low temperature forms of Li_5FeO_4 in the system of Li_2O and Fe_2O_3 [12]. It is reported that the theoretical capacity of Li_5FeO_4 (Mr:155) is 173 $mAhg^{-1}$, and it is thought that in the relationship between ant-fluorite and fluorite structures, Li ions in anti-fluorite Li_5FeO_4 occupy the oxygen position in the fluorite type stabilized zirconia. In 1999, Narukawa [13] reported the synthesis of Li_5FeO_4. In his work, Li_5FeO_4 is prepared by a traditional ceramic method from Li_2O and Fe_2O_3. He inferred from the charge and discharge curves of the Li/Li_5FeO_4 cell that the capacity loss of the first discharge is significantly large, which is more than 50%. In our previous work [14], unsatisfactory incapacity of the Li/Li_5FeO_4 cell is also reported, though Li_5FeO_4 is prepared by a novel method. Thus, improving the electrochemical performance of Li_5FeO_4 is a key topic that must be resolved before this material's commerce is available. To the best of our knowledge, there is no paper reporting the doping of Mn in $LiFeO_4$

Besides metal doping, carbon incorporation is though as another main method for enhancing the electrochemical performance of cathode materials. For example, Wang [15] reported the synthesis of $LiFePO_4/C$ prepared from $FeC_2O_4 \cdot 2H_2O$ and LiH_2PO_4 by a solid-state reaction using citric acid as a carbon source, showing a greatly enhanced rate performance and the cyclic stability at room temperature. Gu [16] published his work on the preparation of the composite of $LiFePO_4$-multiwalled carbon nanotubes (MWCNTs) fabricated by a hydrothermal method followed by ball-milling and heat treating, in which MWCNTs are employed as the carbon sources. Based on our work on MWCNTs [17], in this work, for the first time, MWCNTs are incorporated into Li_5FeO_4 with an intention to improve the electrochemical performance of Mn-doped Li_5FeO_4.

In this study, manganese is doped into Li_5FeO_4 desiring to enhance its electrochemical performance. Herein, the starting materials are $LiOH \cdot H_2O$, $Mn(CH_3COO)_2 \cdot 4H_2O$ and $Fe(NO_3)_3 \cdot 9H_2O$. The molar ratio of Li to the sum of Fe and Mn is 5. That is to say, the molar ratio of Fe to Mn is

slightly altered. But unfortunately, the capacity of the Mn-doped Li_5FeO_4 is also low though the well defined cyclic voltammograms (CVs) of the cell assembled by the Mn-doped Li_5FeO_4 are observed. To promote the conductivity of Li^+ in the cathode materials, the carbon-incorporation method is introduced to promote the electrochemical performance of Mn-doped Li_5FeO_4. The obtained samples are featured thoroughly by XRD patterns, FTIR spectra. The electrochemical performance of the cell comprised of the as-prepared samples is well detected by cyclic voltammetry (CV) and galvanostatic charge-discharge measurement, revealing that the incorporation of CNTs greatly enhanced the electrochemical behavior of $Li_5Fe_{1-x}Mn_xO_4$. It should be mentioned that in this work, the inert gas is not used; instead, a carbon coating protection is employed. And also a two-step calcinations method is utilized.

2. EXPERIMENTAL

2.1. Preparation of Mn-doped Li_5FeO_4

Briefly, stoichiometric amount of $LiOH•H_2O$, $Fe(NO_3)_3•9H_2O$ and $Mn(CH_3COO)_2·4H_2O$ are mixed to give rise to a mixture. And then this mixture is pressed into tablets (the thickness is 0.5mm and the diameter is about 4mm). The tablets are placed in a carbon-coated crucible, here the carbon used are graphite powders. The tablets are heated at a temperature of 470 ^oC for around 10h. And then the obtained samples are ground thoroughly before it is calcinated again at a temperature of 750 ^oC for 3h. It should be mentioned that in this process, the inert gas protection method is not utilized. After cooling down to the room temperature, the resultant powder is thoroughly ground in a mortar. As a result, Li_5FeO_4 is prepared.

In this work, the electrochemical experiments are carried out using the coin-type cells. The working electrode is prepared by mixing active material with poly (tetrafluoroethene) (PTFE) and acetylene black at a weight ratio of 85:10: 5 in N-methyl-2-pyrrolidone (NMP) to form slurry. Then, the resultant slurry is uniformly pasted on an aluminum foil with a blade, dried at 120 °C in a vacuum oven and pressed under a pressure of 20Mpa. The dried foil is transferred to a vacuum oven and kept under 80°C overnight for further drying. The active material loading density of the electrode is ca. 1.0$mg·cm^{-2}$. The Celgard 2400 microporous membrane is used as a separator. Coin type cell is assembled with the cathode as a working electrode and lithium foil as a counter electrode in an N_2-filled glove box. The cells are first charged and then discharged between 2.0V and 4.5V vs. metallic Li with a current density of 0.1C at room temperature. The electrolyte is 1 M $LiClO_4$ in an organic solution (ethylene carbonate, diethyl carbonate and dimethyl carbonate (EC +DEC+DMC) in a volume ratio of 2:5:11 at ambient temperature(25±2°C).

2.2 Characterization

X-ray diffraction (XRD, Germany, Bruker AXS , D8 ADVANCE) analysis of the catalyst is carried out on a Bruker D8ADVANCE X-ray diffractometer equipped with a Cu Kα source (λ =0.154

nm) at 40kV and 30mA.The 2θ angular region between 10 and 90° is recorded at a scan rate of 1°/step. Fourier transform infrared spectrometry (FT-IR) measurements are carried out on a Hitachi FT-IR-8900 spectrometer (Japan). The particle morphology is observed by SEM (HITACHI, S-570).

3. RESULTS AND DISCUSSION

3.1 Characterization of the Mn-doped Li_5FeO_4

FTIR spectra for the samples containing different contents of Mn is shown in Fig.1, it can be seen that see that with the content increase of Mn, the shape of all curves remained unchanged, though the intensity altered slightly. Also, one can see that the intensity of the peaks increased with the increasing of Mn in Li_5FeO_4. Based on the FTIR spectra of $BaFeO_4$ [18], the band centered on 3423cm^{-1} is attributed to stretching and bending vibrations of water. The water may be indraughted during the process of preparing the sample. The band at about 1432cm^{-1} may be the absorption of CO_3^{2-} that may be introduced into the $LiFe_{1-x}Mn_xO_4$ lattice during preparation or the absorbed CO_2 from air. The band centered at the range from 550 cm^{-1} to 1000 cm^{-1} may correspond to the characteristic bands of $LiFe_{1-x}Mn_xO_4$. To our knowledge, this is the first time to display the FTIR spectra of $LiFe_{1-x}Mn_xO_4$. Therefore, one can conclude that the doping of Mn did not affect the main groups in Li_5FeO_4.

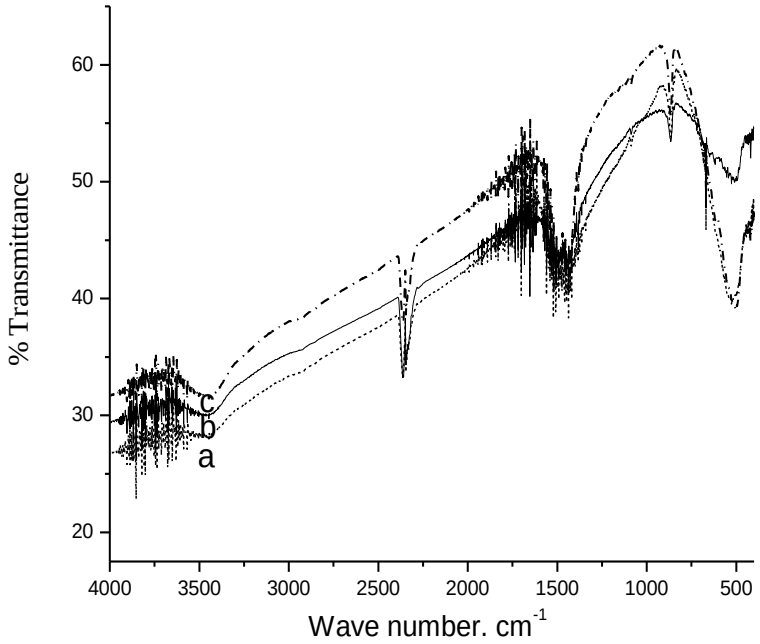

Figure 1. FTIR spectra for the Mn-doped Li_5FeO_4 prepared by a calcination process at 470°C for 10h and at 750°C for 3h from the mixture having LiOH and $Fe(NO_3)_3$ and various content of Mn. Line **a**: $Li_5Fe_{0.95}Mn_{0.05}O_4$; Line **b**: $Li_5Fe_{0.90}Mn_{0.10}O_4$; Line **c:** $Li_5Fe_{0.85}Mn_{0.15}O_4$.

XRD patterns of the Mn-doped Li_5FeO_4 with various content of Mn are shown in Fig.2. One can see that for the sample of $Li_5Fe_{0.85}Mn_{0.15}O_4$ as shown by pattern **c**, more diffraction peaks are observed in comparison with $Li_5Fe_{0.9}Mn_{0.1}O_4$, suggesting that more crystal structures are prepared in the obtained sample. While for $Li_5Fe_{0.90}Mn_{0.10}O_4$, i.e., pattern **b**, instead, the intensity of diffraction peaks located at from 20^{o} to 55^{o} attenuated greatly. It can be seen from Fig.2 that more amount of Mn can change the crystal structure of Li_5FeO_4 obviously.

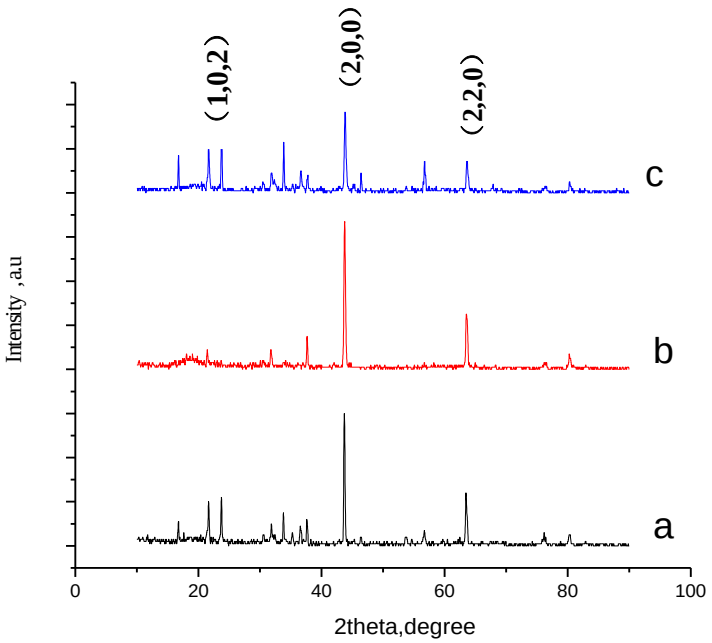

Figure 2. XRD patterns for obtained samples prepared by a calcination process at 470°C for 10h and at 750°C for 3h from the mixture having LiOH and $Fe(NO_3)_3$ with various content of Mn. Pattern **a**:$Li_5Fe_{0.95}Mn_{0.05}O_4$; Pattern **b:** $Li_5Fe_{0.90}Mn_{0.10}O_4$.; pattern **c**: $Li_5Fe_{0.85}Mn_{0.15}O_4$.

Electrochemical Impedance Spectroscopy (EIS) is a powerful technique to record the charge transfer behavior of Li^+ in the cathode materials, thus, the Nyquist plots for the cells assembled by our samples are conducted as shown in Fig.3. According to the previously report[16], the semicircle appearing at the high frequency region corresponds to a circuit having a resistance element parallel to a capacitance element, and generally, a semicircle with a larger diameter corresponds to a larger charge transfer resistance. Thus, approximately, the diameter of the semicircle stands for the value of charge transfer resistance. It seemed that the sample of $Li_5Fe_{0.90}Mn_{0.10}O_4$ showed the smallest resistance among those three samples. While, for the sample of $Li_5Fe_{0.85}Mn_{0.15}O_4$, as shown by line **c**, the charge transfer resistance became larger. Therefore, it can be concluded that the charge transfer resistance altered with the content of Mn correspondingly. Thus, the content of Mn strongly influenced the electrochemical performance of Li_5FeO_4.

The charge-discharge curves for the cell assembled by our prepared samples are also plotted as shown in Fig. 4, where the cell employed is assembled by Mn-doped Li_5FeO_4 with various content of

Mn. The first discharge capacities for $Li_5Fe_{0.95}Mn_{0.05}O_4$; $Li_5Fe_{0.90}Mn_{0.10}O_4$ and $Li_5Fe_{0.85}Mn_{0.15}O_4$ are 14, 21.5 and 17.8mAh/g, respectively. And the sample of $Li_5Fe_{0.90}Mn_{0.10}O_4$ showed the largest discharge capacity, showing the best electrochemical performance among those three samples. But we do admit that the discharge capacity value of the as-prepared sample is lower than the published data [19], probably due to the various preparation conditions or the different measuring conditions.

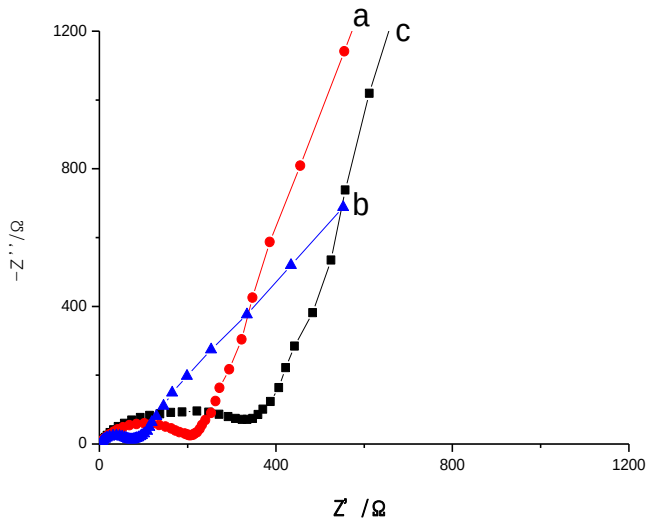

Figure 3. Nyquist plots for the cell assembled by Mn-doped Li_5FeO_4 prepared by a calcination process at 470°C for 10h and at 750°C for 3h from the mixture having LiOH and $Fe(NO_3)_3$ and various content Mn. Pattern **a:** $Li_5Fe_{0.95}$ Mn $_{0.05}O_4$ **;** Pattern **b**: $Li_5Fe_{0.90}$ Mn $_{0.10}O_4$; pattern **c**: $Li_5Fe_{0.85}$ Mn $_{0.15}O_4$.

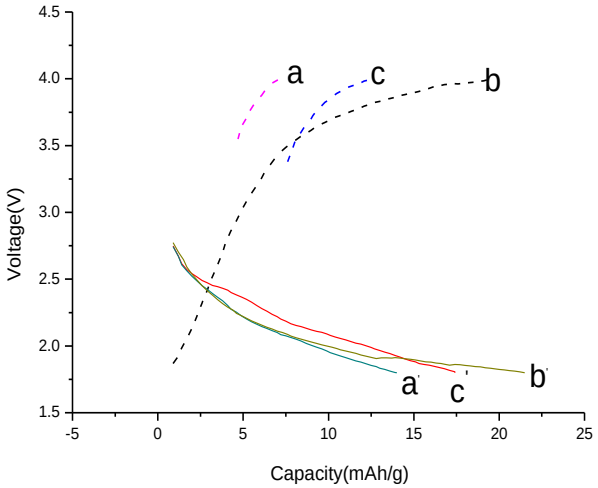

Figure 4. The first charge/discharge curves at 0.1C for the Mn-doped Li_5FeO_4 prepared by a calcination process at 470°C for 10h and at 750°C for 3h from the mixture having LiOH and $Fe(NO_3)_3$ with various content of Mn. Pattern **a**: $Li_5Fe_{0.95}Mn_{0\ .05}O_4$; Pattern **b:** $Li_5Fe_{0.90}Mn_{0.10}O_4$; pattern **c**: $Li_5Fe_{0.85}Mn_{0.15}O_4$.

3.2 Characterization of the CNTs-incorporated $Li_5Fe_{0.90}Mn_{0.10}O_4$

To improve the conductivity of the obtained materials, carbon nanotubes are doped into the precursors of the $Li_5Fe_{0.90}Mn_{0.10}O_4$. Here, three kinds of samples having various contents of CNTs are prepared. Four curves of FTIR spectra corresponding to the four kinds of samples are shown in Fig.5. It can be seen that with the increasing of CNTs contents, the intensities of all curves changed correspondingly. It seemed that the intensity of the FTIR curve increased with the content of CNTs. One can also draw a conclusion that the main shape of all FTIR curves is not affected by the incorporation of CNTs. That is to say, the molecular structure of Li_5FeO_4 is not much affected by the incorporated CNTs.

Fig.6 is the XRD patterns for the as-prepared CNTs-incorporated $Li_5Fe_{0.90}Mn_{0.10}O_4$, in which the content of CNTs in the precursors of $Li_5Fe_{0.90}Mn_{0.10}O_4$ are 3, 6, 9 and 12 wt%, respectively. It can be seen that the intensity of all diffraction peaks are greatly affected by the content of CNTs. For example, the intensity of the diffraction peak at around 30^o for the sample having CNTs 12wt% is enhanced obviously when compared to the sample having lower content of CNTs. While, the peak at about 15^o is evidently attenuated, suggesting that the content of CNTs in the precursors of as-prepared sample is a main factor influencing the crystal structure of prepared samples, though CNTs can not change the main groups in the samples as verified by above FTIR spectra. Referred to the literature [19], pattern **b** is more similar to the standard pattern of Li_5FeO_4

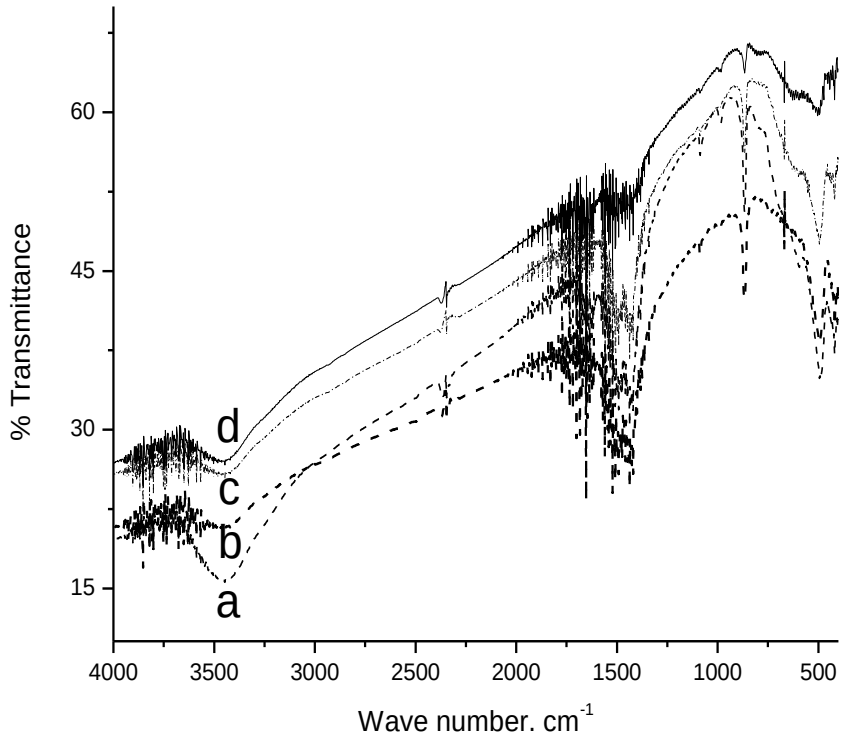

Figure 5. FTIR spectra for the CNTs-incorporated $Li_5Fe_{0.90}Mn_{10}O_4$ prepared by a calcination process at 470°C for 10h and at 750°C for 3h from the mixture having LiOH and $Fe(NO_3)_3$ and $Mn(CH_3COO)_2 \cdot 4H_2O$ various content of CNTs . Line **a**: 3% ; Line **b**: 6%; Line **c**:9% Line **d:12**% .

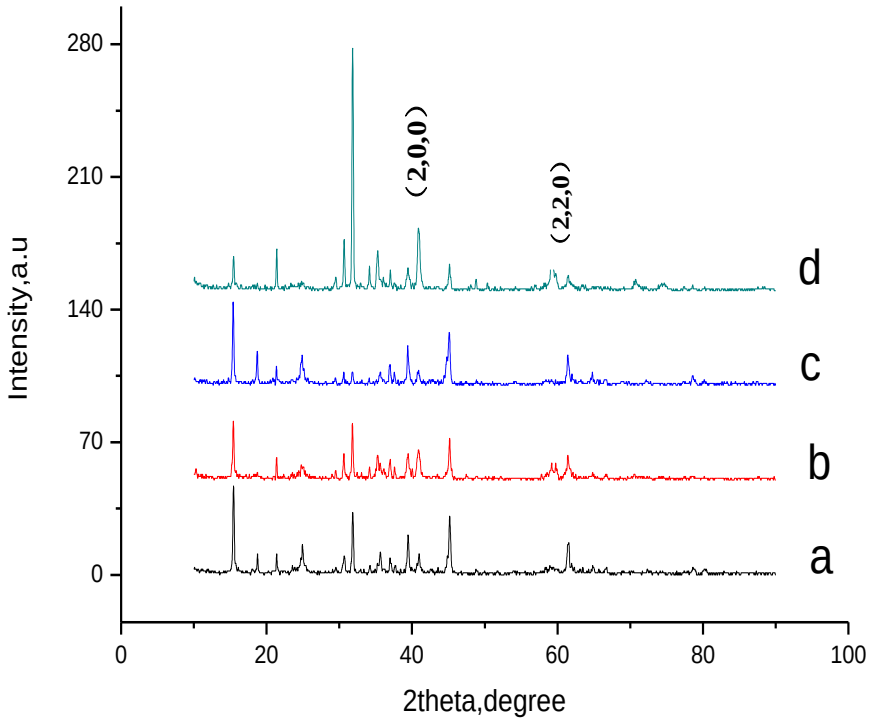

Figure 6. XRD patterns for the CNT-incorporated $Li_5Fe_{0.90}Mn_{0.10}O_4$ prepared by a calcination process at 470°C for 10h and at 750°C for 3h from the mixture having LiOH and $Fe(NO_3)_3$ with $Mn(CH_3COO)_2{\cdot}4H_2O$ and various content of CNTs(wt%). Line **a**: 3%; Line **b:** 6%; pattern **c**: 9%, Line **d**: 12%

Nyquist plots for the cell assembled by the CNTs-incorporated $Li_5Fe_{0.90}Mn_{0.10}O_4$ as the cathode material are shown in Fig.7. One can see that the shape of the semicircle appearing at the high frequency regions is different from each other when the content of CNTs is various. The smallest semicircle is observed for the sample incorporated with 9 wt% CNTs. Interestingly, when the content of CNTs is 12%, a large bow-shaped curve along with a large 45^o line is observed. Therefore, one can conclude that the content of CNTs is a key factor that can influence the electrochemical performance of the obtained samples.

To directly compare the electrochemical performance among the as-prepared samples, the galvanostatic cycling performance, i.e., the charge-discharge curves, of the half battery assembled by the CNTs-incorporated $Li_5Fe_{0.90}Mn_{0.10}O_4$ are shown in Fig.8. In Fig. 8, the charge-discharge rate is 0.1C, the line **a**, **b**, **c** and **d** correspond to the 3, 6, 9 and 12% CNTs-incorporated $Li_5Fe_{0.90}Mn_{0.10}O_4$, respectively.

The first discharge capacities are 30.0, 30.7, 57.7 and 22.5 mAh/g, respectively, for line **a**, **b, c** and **d.** That is to say, the largest value of first discharge capacity is exhibited by the 9wt% CNTs-incorporated $Li_5Fe_{0.90}Mn_{0.10}O_4$, which is consistent with the results shown in the Nyquist plot as shown in Fig.7 very well. More importantly, we conclude that the concept, that more CNTs the cathode material has, better electrochemical performance can be displayed, is not correct, as is proposed for the first time.

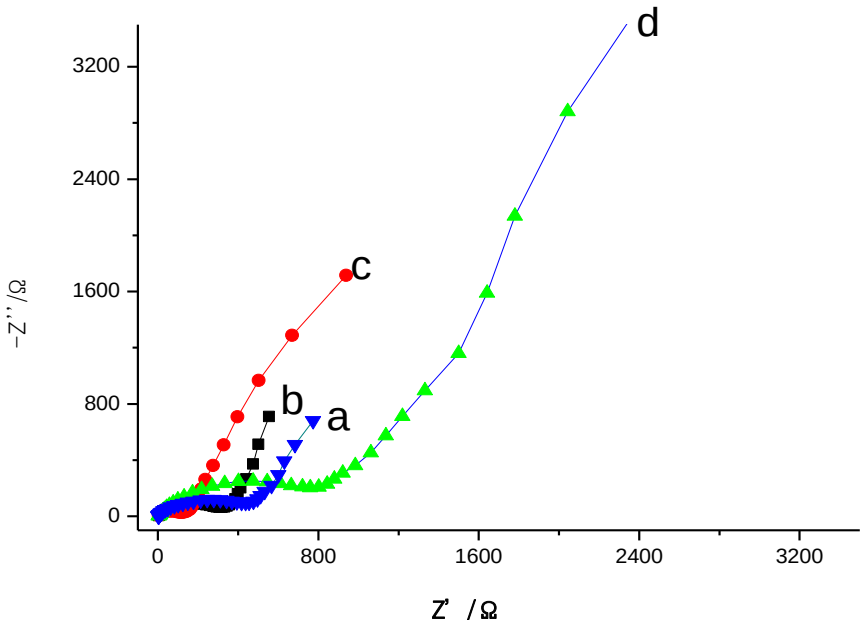

Figure 7. Nyquist plots for the CNTs-incorporated $Li_5Fe_{0.90}Mn_{0.10}O_4$ prepared by a calcination process at 470°C for 10h and at 750°C for 3h from the mixture having LiOH, $Fe(NO_3)_3$ and $Mn(CH_3COO)_2 \cdot 4H_2O$ with various content of CNTs (w%). Line **a**: 3% ; Line **b:** 6%; Line **c**: 9%; Line **d**: 12% .

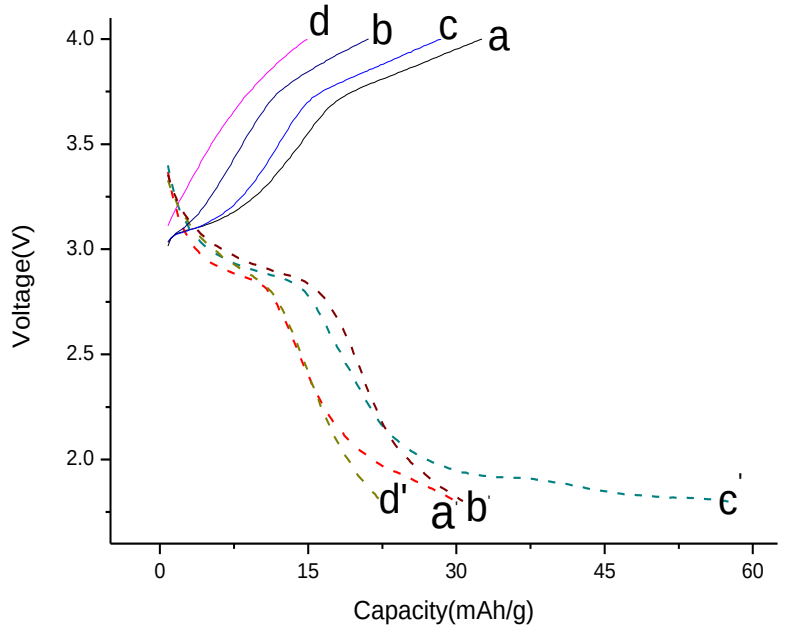

Figure 8. The first charge / first discharge curves (0.1C) for the CNT-incorporated $Li_5Fe_{0.90}Mn_{0.10}O_4$ prepared by a calcination process at 470°C for 10h and at 750°C for 3h from the mixture having LiOH and $Fe(NO_3)_3$ with $Mn(CH_3COO)_2 \cdot 4H_2O$ and various content (w%) of CNT. line **a**: 3%; line **b:** 6%; line **c**: 9% ; line **d**: 12% .

Cyclic voltammograms (CVs) of the cell comprised with the as-prepared sample, i.e., 9% CNTs-incorporated $Li_5Fe_{0.90}Mn_{0.10}O_4$ at various scan rates are t are shown in Fig.9. It can be seen that there is a pair of redox peaks appearing the potential range from 1.5V to 4.3V, indicating that Li^+ can freely extract (charging) /insert (discharging) from /in the cathode materials. And the reduction peak (at around 2.8V) and oxidation peak(at about 3.2V) correspond to the discharging and charging process, respectively. This agrees with the charge-discharge curves shown in Fig. 8 very well. Meanwhile, one can see CVs at scan rate of 0.5mV/s shown by curve **b** is similar to that obtained at 1mV/s. While, when the scan rate is as low as 0.1mV/s, the shape of the CVs changed greatly as shown by curve **c** in Fig.9. Novel redox peaks are appearing at around 3.9V versus Li/Li^+. Probably, when the scan rate is lower, novel phase transitions took placed.

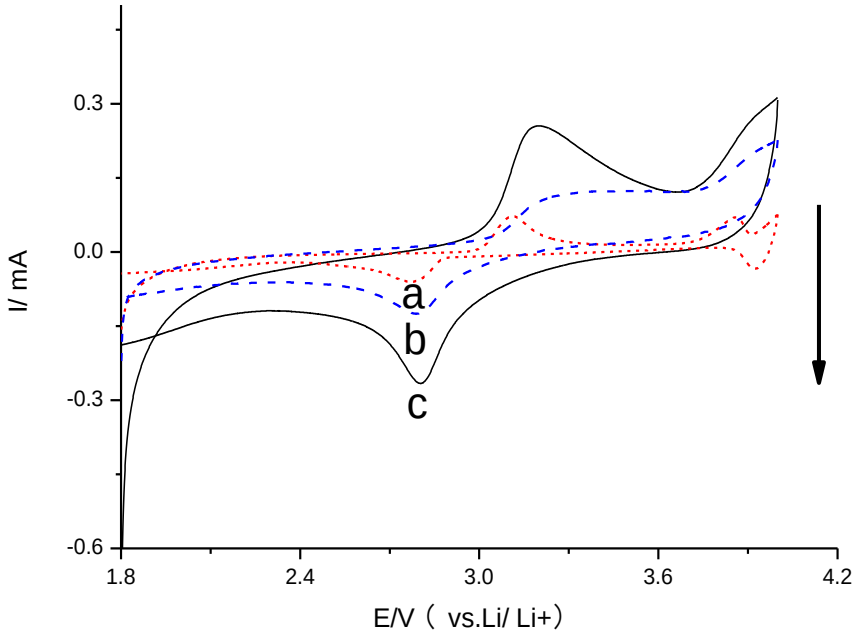

Figure 9. CV for the CNTs-incorporated $Li_5Fe_{0.90}Mn_{0.10}O_4$ prepared by a calcination process at 470°C for 10h and at 750°C for 3h from the mixture having LiOH and $Fe(NO_3)_3$ with $Mn(CH_3COOH)_2 \cdot 4H_2O$ at various scanning rates, a: 0.1 mV/s . b: 0.5mV/s . c: 1mV/s . The content of CNTs (w%) is 9%.

In order to discuss the role of CNTs in the preparing CNTs-incorporated $Li_5Fe_{0.90}Mn_{0.10}O_4$, SEM images of CNTs-incorporated $Li_5Fe_{0.90}Mn_{0.10}O_4$ with various contents of CNTs are shown in Fig.10. To our surprise, it is revealed by Fig.10 that the content of CNTs in the precursors is a key parameter directly influencing the particle size of the obtained samples. It can be seen clearly that the smallest particles are observed as the content of CNTs is 9%. The previous work has demonstrated that the shape and particle size are main factors affecting the electrochemical performance of the cathode materials [20]. Thus, 9% CNTs-incorporated $Li_5Fe_{0.90}Mn_{0.10}O_4$ should deliver the maximum discharge capacity, as is well supported by the charge-discharge curves as shown in Fig.8. As reported, small particle size can shorten the length of Li+ diffusion process [20], thus, leading to an increased

conductivity of Li+ in the cathode materials. But how did the incorporated CNTs affect the conductivity of CNTs-incorporated $Li_5Fe_{0.90}Mn_{0.10}O_4$? How did the incorporated CNTs influence the morphologies of the CNTs-incorporated $Li_5Fe_{0.90}Mn_{0.10}O_4$? What did happen to CNTs in the sintering process? More problems should be resolved in the following works.

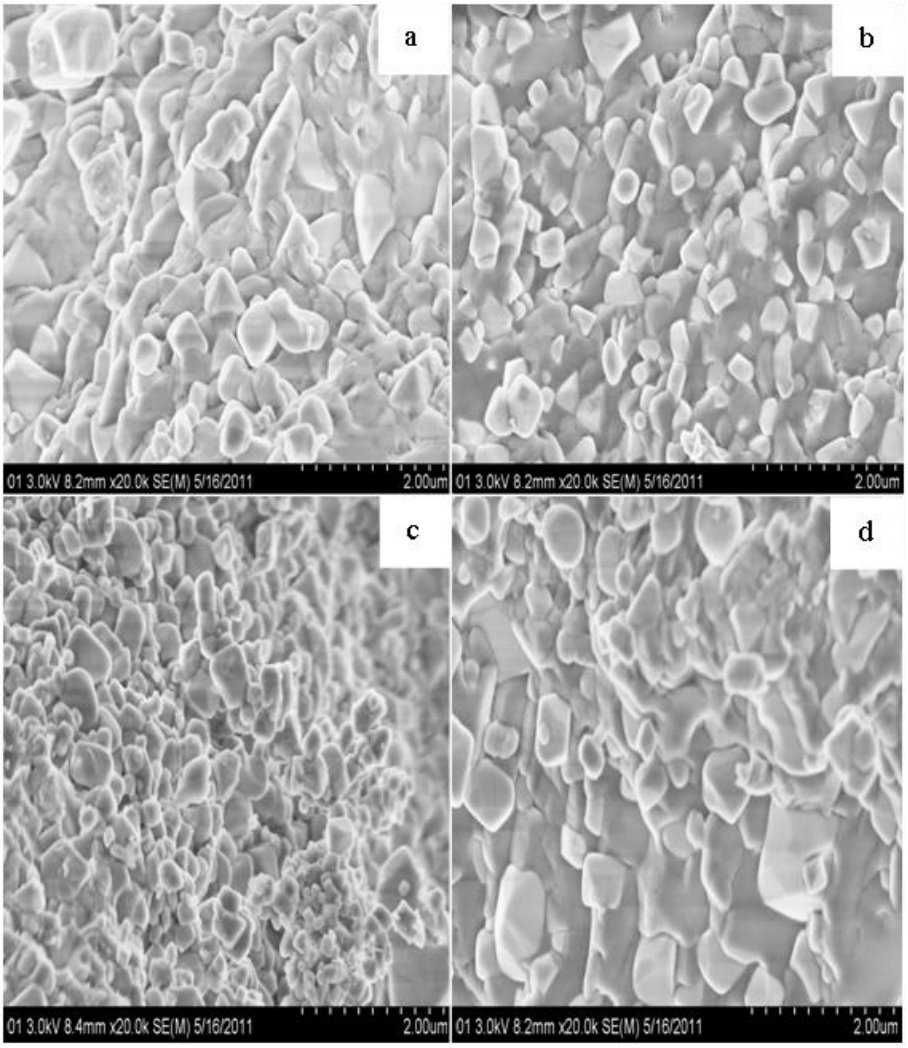

Figure 10. SEM images of the CNT-incorporated $Li_5Fe_{0.90}Mn_{0.10}O_4$ prepared by a calcination process at 470°C for 10h and at 750°C for 3h from the mixture having LiOH and $Fe(NO_3)_3$ with $Mn(CH_3COO)_2 \cdot 4H_2O$ with various content of CNTs . Line **a**: 3% ; Line **b:6**%; Line **c**:9% Line **d**: 12% .

4. CONCLUSIONS

Summarily, the following conclusions are achieved. (1) The content of Mn in Li_5FO_4 has an evident influence on the electrochemical performance of Mn-doped Li_5FeO_4, as is verified by the EIS and galvanostatic charge-discharge measurement. (2) Nyquist plots of EIS also proved that CNTs-incorporated $Li_5Fe_{0.9}Mn_{0.1}O_4$ having 9 wt% CNTs displayed the best charge-discharge performance.

(3) It is proved that the content of CNTs in $Li_5Fe_{1-x}Mn_xO_4$ can not only influence the particles size of obtained samples but also can affect the electrochemical performance. More works should be done to present a satisfactory product of CNTs-incorporated $Li_5Fe_{1-x}Mn_xO_4$

ACKNOWLEDGEMENTS
This work is supported by the Ministry of Science and Technology (Grant No. 2011CB935902 and Grant No. 2010DFA72760), the National Natural Science Foundation of China (Grand No.20901046), the Tsinghua University Initiative Scientific Research Program (Grand No. 2010THZ08116) and Natural Science Foundation of Hebei Province of China (Grant No. B2011205014).

References

1. D. Jugovic′, D. Uskokovic′, *J. Power Sources* 190 (2009) 538–544.
2. C. Sun, S. Rajasekhara, J. B. Goodenough, F. Zhou, *J. Am. Chem. Soc.*, 2011, *133* (7)2132–2135.
3. L. Zhang, X.L. Wang, J.Y. Xiang, Y. Zhou, S.J. Shi, J.P. Tu, *J. Power Sources* 195 (2010) 5057–5061.
4. F. Nobili , S. Dsoke, F. Croce, R. Marassi, *Electrochim.Acta*50(2005)2307–2313.
5. S.-H. Wu, M.-S. Chen , C.-J. Chien , Y.-P. Fu, *J. Power Sources* 189 (2009) 440–444.
6. T. Shiratsuchi, S. Okada, T. Doi, J.-I. Yamaki, *Electrochim. Acta* 54 (2009) 3145–3151.
7. Ni, L. Gao, *J. Power Sources* 196 (2011) 6498–6501.
8. J.-K. Kim , G. S. Chauhan, J.-H. Ahn, H.-J. Ahn, *J. Power Sources* 189 (2009) 391–396.
9. T. Nedoseykina, M. G. Kim, S.-A. Park , H.-S. Kim , S.-B. Kim, J. Cho , Y. Lee, *Electrochim. Acta* 55 (2010) 8876–8882.
10. M. Bini, S. Ferrari, D. Capsoni, V. Massarotti, *Electrochim. Acta* 56 (2011) 2648–2655.
11. I.Saadoune, M. Labrini, M. Yahya , A. Almaggoussi, H. Ehrenberg, *Electrochim. Acta* 55 (2010) 5180–5185.
12. G. Demoisson, F. Jeannot, C. Gleizer, J. Aubry, *C. R. Acad. Sci. Paris* 272 (1971) 458.
13. S. Narukawa, Y Takeda, M. Nishijima, N. Imanishi, O. Yamamoto, M Tabuchi, *Solid State Ionics* 122 (1999) 59.
14. K. Ding , L. Wang , J. Li , H. Jia , X. He, *Int. J. Electrochem. Sci.*, 6 (2011) 2859 – 2868.
15. X.Yan , G. Yang , J. Liu , Y. Ge , H. Xie, X. Pan , R. Wang, *Electrochim. Acta* 54 (2009) 5770–5774.
16. Bo Jin , En Mei Jin , K.-H. Park , H.-B. Gu, *Electrochem. Commun*. 10 (2008) 1537–1540.
17. K. Ding, W. Cai, Q. Wang, Russ. *J. Electrochem.*, 46(2010)180–187.
18. W. Yang , J. Wang, T. Pan , F. Cao, J. Zhang , C.-N. Cao, *Electrochim. Acta* 49(2004)3455–3461.
19. N. Imanishi, Y. Inoue , A. Hirano, M. Ueda , Y. Takeda , H. Sakaebe , M. Tabuchi, *J. Power Sources*146(2005)21–26.
20. M. Gaberscek , R. Dominko, J. Jamnik, *Electrochem. Commun*. 9 (2007) 2778.